Study of $B \to \pi\ell\nu$ and $B \to \rho\ell\nu$ decays and determination of $|V_{ub}|$

B. Aubert,[1] R. Barate,[1] D. Boutigny,[1] F. Couderc,[1] Y. Karyotakis,[1] J. P. Lees,[1] V. Poireau,[1] V. Tisserand,[1] A. Zghiche,[1]
E. Grauges,[2] A. Palano,[3] M. Pappagallo,[3] A. Pompili,[3] J. C. Chen,[4] N. D. Qi,[4] G. Rong,[4] P. Wang,[4] Y. S. Zhu,[4] G. Eigen,[5]
I. Ofte,[5] B. Stugu,[5] G. S. Abrams,[6] M. Battaglia,[6] A. B. Breon,[6] D. N. Brown,[6] J. Button-Shafer,[6] R. N. Cahn,[6] E. Charles,[6]
C. T. Day,[6] M. S. Gill,[6] A. V. Gritsan,[6] Y. Groysman,[6] R. G. Jacobsen,[6] R. W. Kadel,[6] J. Kadyk,[6] L. T. Kerth,[6]
Yu. G. Kolomensky,[6] G. Kukartsev,[6] G. Lynch,[6] L. M. Mir,[6] P. J. Oddone,[6] T. J. Orimoto,[6] M. Pripstein,[6] N. A. Roe,[6]
M. T. Ronan,[6] W. A. Wenzel,[6] M. Barrett,[7] K. E. Ford,[7] T. J. Harrison,[7] A. J. Hart,[7] C. M. Hawkes,[7] S. E. Morgan,[7]
A. T. Watson,[7] M. Fritsch,[8] K. Goetzen,[8] T. Held,[8] H. Koch,[8] B. Lewandowski,[8] M. Pelizaeus,[8] K. Peters,[8] T. Schroeder,[8]
M. Steinke,[8] J. T. Boyd,[9] J. P. Burke,[9] N. Chevalier,[9] W. N. Cottingham,[9] M. P. Kelly,[9] T. Cuhadar-Donszelmann,[10]
B. G. Fulsom,[10] C. Hearty,[10] N. S. Knecht,[10] T. S. Mattison,[10] J. A. McKenna,[10] A. Khan,[11] P. Kyberd,[11] M. Saleem,[11]
L. Teodorescu,[11] A. E. Blinov,[12] V. E. Blinov,[12] A. D. Bukin,[12] V. P. Druzhinin,[12] V. B. Golubev,[12] E. A. Kravchenko,[12]
A. P. Onuchin,[12] S. I. Serednyakov,[12] Yu. I. Skovpen,[12] E. P. Solodov,[12] A. N. Yushkov,[12] D. Best,[13] M. Bondioli,[13]
M. Bruinsma,[13] M. Chao,[13] I. Eschrich,[13] D. Kirkby,[13] A. J. Lankford,[13] M. Mandelkern,[13] R. K. Mommsen,[13]
W. Roethel,[13] D. P. Stoker,[13] C. Buchanan,[14] B. L. Hartfiel,[14] S. D. Foulkes,[15] J. W. Gary,[15] O. Long,[15] B. C. Shen,[15]
K. Wang,[15] L. Zhang,[15] D. del Re,[16] H. K. Hadavand,[16] E. J. Hill,[16] D. B. MacFarlane,[16] H. P. Paar,[16] S. Rahatlou,[16]
V. Sharma,[16] J. W. Berryhill,[17] C. Campagnari,[17] A. Cunha,[17] B. Dahmes,[17] T. M. Hong,[17] M. A. Mazur,[17] J. D. Richman,[17]
W. Verkerke,[17] T. W. Beck,[18] A. M. Eisner,[18] C. J. Flacco,[18] C. A. Heusch,[18] J. Kroseberg,[18] W. S. Lockman,[18] G. Nesom,[18]
T. Schalk,[18] B. A. Schumm,[18] A. Seiden,[18] P. Spradlin,[18] D. C. Williams,[18] M. G. Wilson,[18] J. Albert,[19] E. Chen,[19]
G. P. Dubois-Felsmann,[19] A. Dvoretskii,[19] D. G. Hitlin,[19] I. Narsky,[19] T. Piatenko,[19] F. C. Porter,[19] A. Ryd,[19] A. Samuel,[19]
R. Andreassen,[20] S. Jayatilleke,[20] G. Mancinelli,[20] B. T. Meadows,[20] M. D. Sokoloff,[20] F. Blanc,[21] P. Bloom,[21] S. Chen,[21]
W. T. Ford,[21] U. Nauenberg,[21] A. Olivas,[21] P. Rankin,[21] W. O. Ruddick,[21] J. G. Smith,[21] K. A. Ulmer,[21] S. R. Wagner,[21]
J. Zhang,[21] A. Chen,[22] E. A. Eckhart,[22] A. Soffer,[22] W. H. Toki,[22] R. J. Wilson,[22] Q. Zeng,[22] D. Altenburg,[23] E. Feltresi,[23]
A. Hauke,[23] B. Spaan,[23] T. Brandt,[24] J. Brose,[24] M. Dickopp,[24] V. Klose,[24] H. M. Lacker,[24] R. Nogowski,[24] S. Otto,[24]
A. Petzold,[24] G. Schott,[24] J. Schubert,[24] K. R. Schubert,[24] R. Schwierz,[24] J. E. Sundermann,[24] D. Bernard,[25]
G. R. Bonneaud,[25] P. Grenier,[25] S. Schrenk,[25] Ch. Thiebaux,[25] G. Vasileiadis,[25] M. Verderi,[25] D. J. Bard,[26] P. J. Clark,[26]
W. Gradl,[26] F. Muheim,[26] S. Playfer,[26] Y. Xie,[26] M. Andreotti,[27] V. Azzolini,[27] D. Bettoni,[27] C. Bozzi,[27] R. Calabrese,[27]
G. Cibinetto,[27] E. Luppi,[27] M. Negrini,[27] L. Piemontese,[27] F. Anulli,[28] R. Baldini-Ferroli,[28] A. Calcaterra,[28]
R. de Sangro,[28] G. Finocchiaro,[28] P. Patteri,[28] I. M. Peruzzi,[28,*] M. Piccolo,[28] A. Zallo,[28] A. Buzzo,[29] R. Capra,[29]
R. Contri,[29] M. Lo Vetere,[29] M. Macri,[29] M. R. Monge,[29] S. Passaggio,[29] C. Patrignani,[29] E. Robutti,[29] A. Santroni,[29]
S. Tosi,[29] S. Bailey,[30] G. Brandenburg,[30] K. S. Chaisanguanthum,[30] M. Morii,[30] E. Won,[30] J. Wu,[30] R. S. Dubitzky,[31]
U. Langenegger,[31] J. Marks,[31] S. Schenk,[31] U. Uwer,[31] W. Bhimji,[32] D. A. Bowerman,[32] P. D. Dauncey,[32] U. Egede,[32]
R. L. Flack,[32] J. R. Gaillard,[32] G. W. Morton,[32] J. A. Nash,[32] M. B. Nikolich,[32] G. P. Taylor,[32] W. P. Vazquez,[32]
M. J. Charles,[33] W. F. Mader,[33] U. Mallik,[33] A. K. Mohapatra,[33] J. Cochran,[34] H. B. Crawley,[34] V. Eyges,[34] W. T. Meyer,[34]
S. Prell,[34] E. I. Rosenberg,[34] A. E. Rubin,[34] J. Yi,[34] N. Arnaud,[35] M. Davier,[35] X. Giroux,[35] G. Grosdidier,[35] A. Höcker,[35]
F. Le Diberder,[35] V. Lepeltier,[35] A. M. Lutz,[35] A. Oyanguren,[35] T. C. Petersen,[35] M. Pierini,[35] S. Plaszczynski,[35]
S. Rodier,[35] P. Roudeau,[35] M. H. Schune,[35] A. Stocchi,[35] G. Wormser,[35] C. H. Cheng,[36] D. J. Lange,[36] M. C. Simani,[36]
D. M. Wright,[36] A. J. Bevan,[37] C. A. Chavez,[37] J. P. Coleman,[37] I. J. Forster,[37] J. R. Fry,[37] E. Gabathuler,[37] R. Gamet,[37]
K. A. George,[37] D. E. Hutchcroft,[37] R. J. Parry,[37] D. J. Payne,[37] K. C. Schofield,[37] C. Touramanis,[37] C. M. Cormack,[38]
F. Di Lodovico,[38] R. Sacco,[38] C. L. Brown,[39] G. Cowan,[39] H. U. Flaecher,[39] M. G. Green,[39] D. A. Hopkins,[39]
P. S. Jackson,[39] T. R. McMahon,[39] S. Ricciardi,[39] F. Salvatore,[39] D. Brown,[40] C. L. Davis,[40] J. Allison,[41] N. R. Barlow,[41]
R. J. Barlow,[41] M. C. Hodgkinson,[41] G. D. Lafferty,[41] M. T. Naisbit,[41] J. C. Williams,[41] C. Chen,[42] A. Farbin,[42]
W. D. Hulsbergen,[42] A. Jawahery,[42] D. Kovalskyi,[42] C. K. Lae,[42] V. Lillard,[42] D. A. Roberts,[42] G. Simi,[42] G. Blaylock,[43]
C. Dallapiccola,[43] S. S. Hertzbach,[43] R. Kofler,[43] V. B. Koptchev,[43] X. Li,[43] T. B. Moore,[43] S. Saremi,[43] H. Staengle,[43]
S. Willocq,[43] R. Cowan,[44] K. Koeneke,[44] G. Sciolla,[44] S. J. Sekula,[44] M. Spitznagel,[44] F. Taylor,[44] R. K. Yamamoto,[44]
H. Kim,[45] P. M. Patel,[45] S. H. Robertson,[45] A. Lazzaro,[46] V. Lombardo,[46] F. Palombo,[46] J. M. Bauer,[47] L. Cremaldi,[47]
V. Eschenburg,[47] R. Godang,[47] R. Kroeger,[47] J. Reidy,[47] D. A. Sanders,[47] D. J. Summers,[47] H. W. Zhao,[47] S. Brunet,[48]
D. Côté,[48] P. Taras,[48] B. Viaud,[48] H. Nicholson,[49] N. Cavallo,[50,†] G. De Nardo,[50] F. Fabozzi,[50,†] C. Gatto,[50] L. Lista,[50]
D. Monorchio,[50] P. Paolucci,[50] D. Piccolo,[50] C. Sciacca,[50] M. Baak,[51] H. Bulten,[51] G. Raven,[51] H. L. Snoek,[51] L. Wilden,[51]
C. P. Jessop,[52] J. M. LoSecco,[52] T. Allmendinger,[53] G. Benelli,[53] K. K. Gan,[53] K. Honscheid,[53] D. Hufnagel,[53]
P. D. Jackson,[53] H. Kagan,[53] R. Kass,[53] T. Pulliam,[53] A. M. Rahimi,[53] R. Ter-Antonyan,[53] Q. K. Wong,[53] J. Brau,[54]

R. Frey,[54] O. Igonkina,[54] M. Lu,[54] C. T. Potter,[54] N. B. Sinev,[54] D. Strom,[54] J. Strube,[54] E. Torrence,[54] A. Dorigo,[55] F. Galeazzi,[55] M. Margoni,[55] M. Morandin,[55] M. Posocco,[55] M. Rotondo,[55] F. Simonetto,[55] R. Stroili,[55] C. Voci,[55] M. Benayoun,[56] H. Briand,[56] J. Chauveau,[56] P. David,[56] L. Del Buono,[56] Ch. de la Vaissière,[56] O. Hamon,[56] M. J. J. John,[56] Ph. Leruste,[56] J. Malclès,[56] J. Ocariz,[56] L. Roos,[56] G. Therin,[56] P. K. Behera,[57] L. Gladney,[57] Q. H. Guo,[57] J. Panetta,[57] M. Biasini,[58] R. Covarelli,[58] S. Pacetti,[58] M. Pioppi,[58] C. Angelini,[59] G. Batignani,[59] S. Bettarini,[59] F. Bucci,[59] G. Calderini,[59] M. Carpinelli,[59] R. Cenci,[59] F. Forti,[59] M. A. Giorgi,[59] A. Lusiani,[59] G. Marchiori,[59] M. Morganti,[59] N. Neri,[59] E. Paoloni,[59] M. Rama,[59] G. Rizzo,[59] J. Walsh,[59] M. Haire,[60] D. Judd,[60] D. E. Wagoner,[60] J. Biesiada,[61] N. Danielson,[61] P. Elmer,[61] Y. P. Lau,[61] C. Lu,[61] J. Olsen,[61] A. J. S. Smith,[61] A. V. Telnov,[61] F. Bellini,[62] G. Cavoto,[62] A. D'Orazio,[62] E. Di Marco,[62] R. Faccini,[62] F. Ferrarotto,[62] F. Ferroni,[62] M. Gaspero,[62] L. Li Gioi,[62] M. A. Mazzoni,[62] S. Morganti,[62] G. Piredda,[62] F. Polci,[62] F. Safai Tehrani,[62] C. Voena,[62] H. Schröder,[63] G. Wagner,[63] R. Waldi,[63] T. Adye,[64] N. De Groot,[64] B. Franek,[64] G. P. Gopal,[64] E. O. Olaiya,[64] F. F. Wilson,[64] R. Aleksan,[65] S. Emery,[65] A. Gaidot,[65] S. F. Ganzhur,[65] P.-F. Giraud,[65] G. Graziani,[65] G. Hamel de Monchenault,[65] W. Kozanecki,[65] M. Legendre,[65] G. W. London,[65] B. Mayer,[65] G. Vasseur,[65] Ch. Yèche,[65] M. Zito,[65] M. V. Purohit,[66] A. W. Weidemann,[66] J. R. Wilson,[66] F. X. Yumiceva,[66] T. Abe,[67] M. T. Allen,[67] D. Aston,[67] R. Bartoldus,[67] N. Berger,[67] A. M. Boyarski,[67] O. L. Buchmueller,[67] R. Claus,[67] M. R. Convery,[67] M. Cristinziani,[67] J. C. Dingfelder,[67] D. Dong,[67] J. Dorfan,[67] D. Dujmic,[67] W. Dunwoodie,[67] E. E. Elsen,[67] S. Fan,[67] R. C. Field,[67] T. Glanzman,[67] S. J. Gowdy,[67] T. Hadig,[67] V. Halyo,[67] C. Hast,[67] T. Hryn'ova,[67] W. R. Innes,[67] M. H. Kelsey,[67] P. Kim,[67] M. L. Kocian,[67] D. W. G. S. Leith,[67] J. Libby,[67] S. Luitz,[67] V. Luth,[67] H. L. Lynch,[67] H. Marsiske,[67] R. Messner,[67] D. R. Muller,[67] C. P. O'Grady,[67] V. E. Ozcan,[67] A. Perazzo,[67] M. Perl,[67] B. N. Ratcliff,[67] A. Roodman,[67] A. A. Salnikov,[67] R. H. Schindler,[67] J. Schwiening,[67] A. Snyder,[67] J. Stelzer,[67] D. Su,[67] M. K. Sullivan,[67] K. Suzuki,[67] S. Swain,[67] J. M. Thompson,[67] J. Va'vra,[67] M. Weaver,[67] A. J. R. Weinstein,[67] W. J. Wisniewski,[67] M. Wittgen,[67] D. H. Wright,[67] A. K. Yarritu,[67] K. Yi,[67] C. C. Young,[67] P. R. Burchat,[68] A. J. Edwards,[68] S. A. Majewski,[68] B. A. Petersen,[68] C. Roat,[68] M. Ahmed,[69] S. Ahmed,[69] M. S. Alam,[69] J. A. Ernst,[69] M. A. Saeed,[69] F. R. Wappler,[69] S. B. Zain,[69] W. Bugg,[70] M. Krishnamurthy,[70] S. M. Spanier,[70] R. Eckmann,[71] J. L. Ritchie,[71] A. Satpathy,[71] R. F. Schwitters,[71] J. M. Izen,[72] I. Kitayama,[72] X. C. Lou,[72] S. Ye,[72] F. Bianchi,[73] M. Bona,[73] F. Gallo,[73] D. Gamba,[73] M. Bomben,[74] L. Bosisio,[74] C. Cartaro,[74] F. Cossutti,[74] G. Della Ricca,[74] S. Dittongo,[74] S. Grancagnolo,[74] L. Lanceri,[74] L. Vitale,[74] F. Martinez-Vidal,[75] R. S. Panvini,[76,‡] Sw. Banerjee,[77] B. Bhuyan,[77] C. M. Brown,[77] D. Fortin,[77] K. Hamano,[77] R. Kowalewski,[77] J. M. Roney,[77] R. J. Sobie,[77] J. J. Back,[78] P. F. Harrison,[78] T. E. Latham,[78] G. B. Mohanty,[78] H. R. Band,[79] X. Chen,[79] B. Cheng,[79] S. Dasu,[79] M. Datta,[79] A. M. Eichenbaum,[79] K. T. Flood,[79] M. Graham,[79] J. J. Hollar,[79] J. R. Johnson,[79] P. E. Kutter,[79] H. Li,[79] R. Liu,[79] B. Mellado,[79] A. Mihalyi,[79] Y. Pan,[79] R. Prepost,[79] P. Tan,[79] J. H. von Wimmersperg-Toeller,[79] S. L. Wu,[79] Z. Yu,[79] and H. Neal[80]

(*BABAR* Collaboration)

[1]*Laboratoire de Physique des Particules, F-74941 Annecy-le-Vieux, France*
[2]*IFAE, Universitat Autonoma de Barcelona, E-08193 Bellaterra, Barcelona, Spain*
[3]*Università di Bari, Dipartimento di Fisica and INFN, I-70126 Bari, Italy*
[4]*Institute of High Energy Physics, Beijing 100039, China*
[5]*University of Bergen, Institute of Physics, N-5007 Bergen, Norway*
[6]*Lawrence Berkeley National Laboratory and University of California, Berkeley, California 94720, USA*
[7]*University of Birmingham, Birmingham, B15 2TT, United Kingdom*
[8]*Ruhr Universität Bochum, Institut für Experimentalphysik 1, D-44780 Bochum, Germany*
[9]*University of Bristol, Bristol BS8 1TL, United Kingdom*
[10]*University of British Columbia, Vancouver, British Columbia, Canada V6T 1Z1*
[11]*Brunel University, Uxbridge, Middlesex UB8 3PH, United Kingdom*
[12]*Budker Institute of Nuclear Physics, Novosibirsk 630090, Russia*
[13]*University of California at Irvine, Irvine, California 92697, USA*
[14]*University of California at Los Angeles, Los Angeles, California 90024, USA*
[15]*University of California at Riverside, Riverside, California 92521, USA*
[16]*University of California at San Diego, La Jolla, California 92093, USA*
[17]*University of California at Santa Barbara, Santa Barbara, California 93106, USA*
[18]*University of California at Santa Cruz, Institute for Particle Physics, Santa Cruz, California 95064, USA*
[19]*California Institute of Technology, Pasadena, California 91125, USA*
[20]*University of Cincinnati, Cincinnati, Ohio 45221, USA*
[21]*University of Colorado, Boulder, Colorado 80309, USA*
[22]*Colorado State University, Fort Collins, Colorado 80523, USA*

[23]Universität Dortmund, Institut fur Physik, D-44221 Dortmund, Germany

[24]Technische Universität Dresden, Institut für Kern-und Teilchenphysik, D-01062 Dresden, Germany

[25]Ecole Polytechnique, LLR, F-91128 Palaiseau, France

[26]University of Edinburgh, Edinburgh EH9 3JZ, United Kingdom

[27]Università di Ferrara, Dipartimento di Fisica and INFN, I-44100 Ferrara, Italy

[28]Laboratori Nazionali di Frascati dell'INFN, I-00044 Frascati, Italy

[29]Università di Genova, Dipartimento di Fisica and INFN, I-16146 Genova, Italy

[30]Harvard University, Cambridge, Massachusetts 02138, USA

[31]Universität Heidelberg, Physikalisches Institut, Philosophenweg 12, D-69120 Heidelberg, Germany

[32]Imperial College London, London, SW7 2AZ, United Kingdom

[33]University of Iowa, Iowa City, Iowa 52242, USA

[34]Iowa State University, Ames, Iowa 50011-3160, USA

[35]Laboratoire de l'Accélérateur Linéaire, F-91898 Orsay, France

[36]Lawrence Livermore National Laboratory, Livermore, California 94550, USA

[37]University of Liverpool, Liverpool L69 72E, United Kingdom

[38]Queen Mary, University of London, E1 4NS, United Kingdom

[39]University of London, Royal Holloway and Bedford New College, Egham, Surrey TW20 0EX, United Kingdom

[40]University of Louisville, Louisville, Kentucky 40292, USA

[41]University of Manchester, Manchester M13 9PL, United Kingdom

[42]University of Maryland, College Park, Maryland 20742, USA

[43]University of Massachusetts, Amherst, Massachusetts 01003, USA

[44]Massachusetts Institute of Technology, Laboratory for Nuclear Science, Cambridge, Massachusetts 02139, USA

[45]McGill University, Montréal, Quebec, Canada H3A 2T8

[46]Università di Milano, Dipartimento di Fisica and INFN, I-20133 Milano, Italy

[47]University of Mississippi, University, Mississippi 38677, USA

[48]Université de Montréal, Laboratoire René J. A. Lévesque, Montréal, Quebec, Canada H3C 3J7

[49]Mount Holyoke College, South Hadley, Massachusetts 01075, USA

[50]Università di Napoli Federico II, Dipartimento di Scienze Fisiche and INFN, I-80126, Napoli, Italy

[51]NIKHEF, National Institute for Nuclear Physics and High Energy Physics, NL-1009 DB Amsterdam, The Netherlands

[52]University of Notre Dame, Notre Dame, Indiana 46556, USA

[53]Ohio State University, Columbus, Ohio 43210, USA

[54]University of Oregon, Eugene, Oregon 97403, USA

[55]Università di Padova, Dipartimento di Fisica and INFN, I-35131 Padova, Italy

[56]Universités Paris VI et VII, Laboratoire de Physique Nucléaire et de Hautes Energies, F-75252 Paris, France

[57]University of Pennsylvania, Philadelphia, Pennsylvania 19104, USA

[58]Università di Perugia, Dipartimento di Fisica and INFN, I-06100 Perugia, Italy

[59]Università di Pisa, Dipartimento di Fisica, Scuola Normale Superiore and INFN, I-56127 Pisa, Italy

[60]Prairie View A&M University, Prairie View, Texas 77446, USA

[61]Princeton University, Princeton, New Jersey 08544, USA

[62]Università di Roma La Sapienza, Dipartimento di Fisica and INFN, I-00185 Roma, Italy

[63]Universität Rostock, D-18051 Rostock, Germany

[64]Rutherford Appleton Laboratory, Chilton, Didcot, Oxon, OX11 0QX, United Kingdom

[65]DSM/Dapnia, CEA/Saclay, F-91191 Gif-sur-Yvette, France

[66]University of South Carolina, Columbia, South Carolina 29208, USA

[67]Stanford Linear Accelerator Center, Stanford, California 94309, USA

[68]Stanford University, Stanford, California 94305-4060, USA

[69]State University of New York, Albany, New York 12222, USA

[70]University of Tennessee, Knoxville, Tennessee 37996, USA

[71]University of Texas at Austin, Austin, Texas 78712, USA

[72]University of Texas at Dallas, Richardson, Texas 75083, USA

[73]Università di Torino, Dipartimento di Fisica Sperimentale and INFN, I-10125 Torino, Italy

[74]Università di Trieste, Dipartimento di Fisica and INFN, I-34127 Trieste, Italy

[75]IFIC, Universitat de Valencia-CSIC, E-46071 Valencia, Spain

[76]Vanderbilt University, Nashville, Tennessee 37235, USA

[77]University of Victoria, Victoria, British Columbia, Canada V8W 3P6

[78]Department of Physics, University of Warwick, Coventry CV4 7AL, United Kingdom

[*]Also with Università di Perugia, Dipartimento di Fisica, Perugia, Italy

[†]Also with Università della Basilicata, Potenza, Italy

[‡]Deceased

[79]*University of Wisconsin, Madison, Wisconsin 53706, USA*
[80]*Yale University, New Haven, Connecticut 06511, USA*

We present an analysis of exclusive charmless semileptonic *B*-meson decays based on 83×10^6 $B\overline{B}$ pairs recorded with the *BABAR* detector at the $\Upsilon(4S)$ resonance. Using isospin symmetry, we measure branching fractions $\mathcal{B}(B^0 \rightarrow \pi^- \ell^+ \nu) = (1.38 \pm 0.10 \pm 0.16 \pm 0.08) \times 10^{-4}$ and $\mathcal{B}(B^0 \rightarrow \rho^- \ell^+ \nu) = (2.14 \pm 0.21 \pm 0.48 \pm 0.28) \times 10^{-4}$, where the errors are statistical, experimental systematic, and due to form-factor shape uncertainties. We compare the measured distribution in q^2, the momentum-transfer squared, with theoretical predictions for the form factors from lattice QCD and light-cone sum rules, and extract the Cabibbo-Kobayashi-Maskawa (CKM) matrix element $|V_{ub}| = (3.82 \pm 0.14 \pm 0.22 \pm 0.11^{+0.88}_{-0.52}) \times 10^{-3}$ from $B \rightarrow \pi\ell\nu$, where the fourth error reflects the uncertainty of the form-factor normalization.

The parameter $|V_{ub}|$ is one of the smallest and least known elements of the Cabibbo-Kobayashi-Maskawa (CKM) quark-mixing matrix [1]. A precise determination of $|V_{ub}|$ would significantly improve the constraints on the unitarity triangle and provide a stringent test of the standard model mechanism for *CP* violation. In this paper, we present a determination of $|V_{ub}|$ from charmless semileptonic decays of *B* mesons with exclusively reconstructed final states, $B \rightarrow h_u \ell \nu$, where the hadronic state h_u represents a $\pi^{\pm}$, π^0, $\rho^{\pm}$, or ρ^0, and ℓ represents *e* or μ. Exclusive decays allow for kinematic constraints and more efficient background suppression compared to inclusive decays, but must rely on theoretical form-factor predictions. Using isospin symmetry, we measure the branching fractions $\mathcal{B}(B^0 \rightarrow \pi^- \ell^+ \nu)$ [2] and $\mathcal{B}(B^0 \rightarrow \rho^- \ell^+ \nu)$ as a function of $q^2 = (p_\ell + p_\nu)^2$, the momentum-transfer squared, and extract $|V_{ub}|$ using recent form-factor calculations based on light-cone sum rules (LCSR) [3,4] and unquenched lattice QCD (LQCD) [5,6].

This measurement is based on a sample of 83×10^6 $B\overline{B}$ pairs recorded with the *BABAR* detector [7] at the PEP-II asymmetric-energy e^+e^- storage rings. The data correspond to an integrated luminosity of 75.6 fb^{-1} collected at the $\Upsilon(4S)$ resonance and 8.9 fb^{-1} recorded 40 MeV below it. Simulated $B\overline{B}$ events are used to estimate signal efficiencies and shapes of signal and background distributions. Charmless semileptonic decays are simulated as a mixture of three-body decays $B \rightarrow X_u \ell \nu$ ($X_u = \pi, \eta, \eta', \rho, \omega$) based on the ISGW II quark model [8]. Decays to nonresonant hadronic states X_u with masses $m_{X_u} > 2m_\pi$ are simulated following a prescription of Ref. [9].

We identify charmless semileptonic decays by a charged lepton with momentum $|\vec{p}_\ell^*| > 1.3$ GeV [10], a π or ρ meson, and missing momentum $|\vec{p}_{\text{miss}}| > 0.7$ GeV in the event. We identify ρ mesons via the decays $\rho^{\pm} \rightarrow \pi^{\pm} \pi^0$ and $\rho^0 \rightarrow \pi^+ \pi^-$ with mass $0.65 < m_{\pi\pi} < 0.85$ GeV, rejecting candidates in which a charged track is identified as a kaon; both $\pi^{\pm}$ and ρ candidates are rejected if a charged track is identified as a lepton. The charged lepton is combined with a π^0, ρ^0 or $\pi^{\pm}$, $\rho^{\pm}$ of opposite charge to form a

"*Y*" candidate; *Y* candidates are rejected if the lepton and an oppositely charged track from the signal hadron are consistent with a $J/\psi \rightarrow \ell^+ \ell^-$ decay.

The neutrino four-momentum, $p_\nu = (E_{\text{miss}}, \vec{p}_{\text{miss}})$, is inferred from the difference between the net four-momentum of the colliding-beam particles, $p_{\text{beams}} = (E_{\text{beams}}, \vec{p}_{\text{beams}})$, and the sum of the four-momenta of all detected particles in the event. To reduce the effect of losses due to the detector acceptance, we require a total charge of the event of $|Q_{\text{tot}}| \leq 1$ and a polar angle of the missing momentum in the range $0.6 < \theta_{\text{miss}} < 2.9$ rad. In addition, the missing mass measured from the whole event should be compatible with zero. Because the missing-mass resolution varies linearly with the missing energy, we require $|m_{\text{miss}}^2 / 2E_{\text{miss}}| < 0.4$ GeV. We compute the angle between the *Y* candidate and the *B* meson, assuming zero missing mass, as $\cos\theta_{BY} = (2E_B^* E_Y^* - M_B^2 - M_Y^2)/(2|\vec{p}_B^*||\vec{p}_Y^*|)$. Here M_B, M_Y, E_B^*, E_Y^*, $\vec{p}_B^*$, $\vec{p}_Y^*$ refer to the masses, energies, and momenta of the *B* and *Y*. Signal candidates are required to satisfy $|\cos\theta_{BY}| < 1.1$, allowing for detector resolution and photon radiation.

We restrict the momenta of leptons and hadrons in *Y* candidates to enhance the signal over backgrounds. For $B \rightarrow \pi\ell\nu$, we require $|\vec{p}_\ell^*| + |\vec{p}_{h_u}^*| > 2.6$ GeV; for $B \rightarrow \rho\ell\nu$, $1.5|\vec{p}_\ell^*| + |\vec{p}_{h_u}^*| > 4.2$ GeV and $|\vec{p}_\ell^*| > 1.8$ GeV. These criteria keep 99.8% (75%) of true $B \rightarrow \pi(\rho)\ell\nu$ decays and reduce the $B \rightarrow X_c \ell\nu$ background by about 10% (80%) after all other selection criteria. To suppress backgrounds from $e^+e^- \rightarrow q\overline{q}$ ($q = u, d, s, c$) and QED processes, we require at least five charged tracks in each event or, to increase the efficiency for $B^+ \rightarrow \pi^0 \ell^+ \nu$, four tracks and at least two photons. We also require $L_2 = \sum_i |\vec{p}_i^*| \cos^2\theta_i^* < 1.5$ GeV. Here the sum is over all tracks in the event excluding the *Y* candidate, and $\vec{p}_i^*$ and θ_i^* refer to the momenta and the angles measured with respect to the thrust axis of the *Y*. This requirement removes over 95% of $q\overline{q}$ and 80% of $B \rightarrow X_c \ell\nu$ background and retains about 50% of the signal in all modes.

We discriminate against the remaining background using the variables $\Delta E = (p_B \cdot p_{\text{beams}} - s/2)/\sqrt{s}$ and

RAPID COMMUNICATIONS

STUDY OF $B \rightarrow \pi\ell\nu$ AND $B \rightarrow \rho\ell\nu$ DECAYS AND ... PHYSICAL REVIEW D **72,** 051102 (2005)

$m_{\mathrm{ES}} = \sqrt{(s/2 + \vec{p}_B \cdot \vec{p}_{\mathrm{beams}})^2 / E_{\mathrm{beams}}^2 - \vec{p}_B^2}$, where $\sqrt{s}$ is the mass of the $\Upsilon(4S)$. Only candidates with $|\Delta E| < 0.9$ GeV and $m_{\mathrm{ES}} > 5.095$ GeV are retained. The total signal selection efficiencies for the sum of electrons and muons are 3.5% and 2.4% for $\pi^-\ell^+\nu$ and $\pi^0\ell^+\nu$, and 0.53% and 1.1% for $\rho^-\ell^+\nu$ and $\rho^0\ell^+\nu$ [11]. We use a low-background sample of $B^0 \rightarrow D^{*-}\ell^+\nu$ decays with $\overline{D}^0 \rightarrow K^+\pi^-$ or $\overline{D}^0 \rightarrow K^+\pi^-\pi^0$ to compare the efficiencies of each selection cut in data and simulation and find differences typically of a few percent.

To extract the signal yields, we perform a binned extended maximum-likelihood fit [12] to the ΔE vs. m_{ES} distributions of the four signal modes simultaneously. The fit takes into account statistical fluctuations of both data and Monte-Carlo samples. We fit the relative proportions of the simulated signal and background samples to the data distributions in 5 GeV^2 or 10 GeV^2 intervals of q^2. To improve the q^2 resolution, we adjust $|\vec{p}_\nu|$ so that $\Delta E = 0$. The resulting q^2 resolution is small compared to the chosen intervals of q^2 and can be described by the sum of two Gaussian functions of widths $\sigma_1 \simeq 0.2$ GeV^2 (containing about 75% of signal events) and $\sigma_2 \simeq 0.5$ GeV^2.

We use the isospin relations $\Gamma(B^0 \rightarrow \pi^-\ell^+\nu) = 2\Gamma(B^+ \rightarrow \pi^0\ell^+\nu)$ and $\Gamma(B^0 \rightarrow \rho^-\ell^+\nu) = 2\Gamma(B^+ \rightarrow \rho^0\ell^+\nu)$ to reduce the number of fit parameters to nine: five for the signal yields in the five q^2 intervals for $B \rightarrow \pi\ell\nu$ decays, three for the signal yields in the three q^2 intervals for $B \rightarrow \rho\ell\nu$ decays, plus one scale parameter, shared among all q^2 intervals and signal modes, to fit the overall normalization of the $B \rightarrow X_c\ell\nu$ background. We classify signal candidates as "combinatoric signal" if the reconstructed lepton comes from the isospin-conjugate decay or the hadron is incorrectly selected. The fit uses common parameters for combinatoric signal and signal. The normalization of the simulated non-$B\overline{B}$ background is scaled separately for events with $e^\pm$ and $\mu^\pm$ to match the off-resonance data. We smooth the distributions for this low-statistics background to reduce single-bin statistical fluctuations.

Figures 1 and 2 show projections of the fitted ΔE vs. m_{ES} distributions for each q^2 interval for $B \rightarrow \pi\ell\nu$ and $B \rightarrow \rho\ell\nu$, respectively. Integrated over the whole q^2 range, we observe 396 $\pi^-\ell^+\nu$, 137 $\pi^0\ell^+\nu$, 95 $\rho^-\ell^+\nu$, and 98 $\rho^0\ell^+\nu$ decays. The resulting partial and total branching fractions are given in Table I. The fitted normalization of
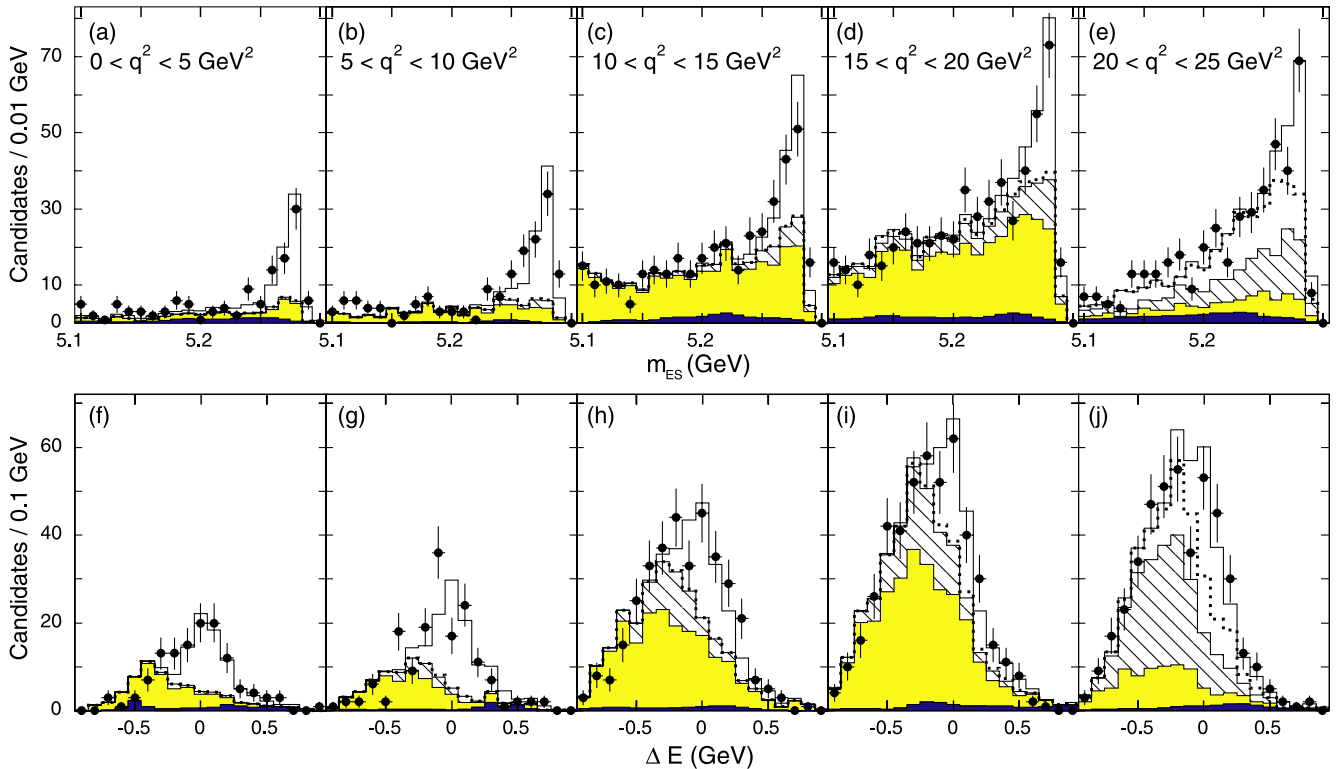
FIG. 1 (color online). Projected m_{ES} (a–e) and ΔE (f–j) distributions in five intervals of q^2 for the combined $B \rightarrow \pi\ell\nu$ modes. The projections are shown for signal bands $-0.15 < \Delta E < 0.25$ GeV and $m_{\mathrm{ES}} > 5.255$ GeV, respectively. The error bars on the data points represent the statistical uncertainties. The histograms show simulated distributions for signal (white), combinatoric signal (white, dotted), cross feed from other $B \rightarrow X_u\ell\nu$ decays (hatched), $B \rightarrow X_c\ell\nu$ decays (light shaded/yellow), and non-$B\overline{B}$ background (dark shaded/blue). The normalizations of the signal and $B \rightarrow X_c\ell\nu$ background simulations have been scaled to the results of the maximum-likelihood fit.
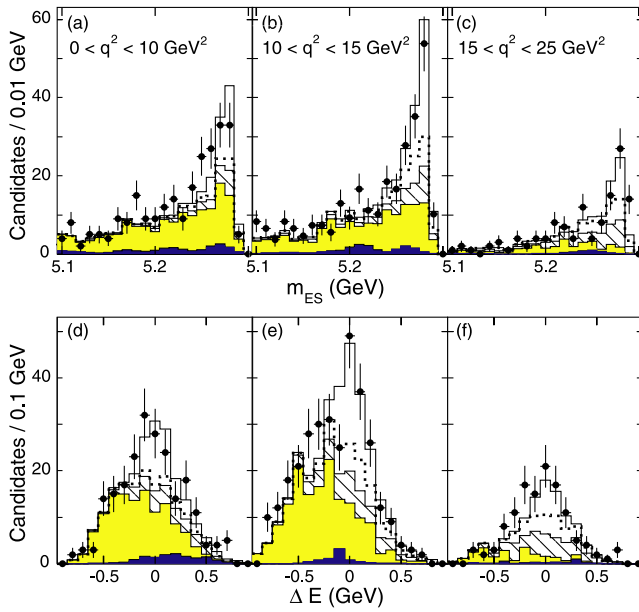
FIG. 2 (color online). Projected m_{ES} (a–c) and ΔE (d–f) distributions in three intervals of q^2 for the combined $B \rightarrow \rho \ell \nu$ modes. See the caption for Fig. 1 for details.

the $B \rightarrow X_c \ell \nu$ background is consistent with the measured total branching fraction [13]. The goodness-of-fit is evaluated using a χ^2-based comparison of the fitted ΔE vs. m_{ES} distributions and data, yielding $\chi^2/\text{dof} = 1.27$. As a check, we have performed the fit for $e^{\pm}$ and $\mu^{\pm}$ separately and obtain consistent results.

The fit also allows us to study the q^2 dependence of the form factors. In decays to pseudoscalar mesons there is only one form factor, f_+ (for low-mass leptons), and we can extract the shape of $f_+(q^2)$ directly from the measured q^2 spectrum. We perform a χ^2 fit with a function proposed by Becirevic and Kaidalov (BK) [14],

$$f_+(q^2) = \frac{c_B(1-\alpha)}{(1 - q^2/m_{B^*}^2)(1 - \alpha q^2/m_{B^*}^2)}, \qquad (1)$$

where $m_{B^*} = 5.32$ GeV is the mass of the B^* resonance, c_B

TABLE I. Partial and total branching fractions $\mathcal{B}(B^0 \rightarrow \pi^- \ell^+ \nu)$ ($\Delta \mathcal{B}_\pi$) and $\mathcal{B}(B^0 \rightarrow \rho^- \ell^+ \nu)$ ($\Delta \mathcal{B}_\rho$) obtained from the simultaneous fit of the four signal modes, and signal efficiencies, ϵ_π and ϵ_ρ, averaged over charged and neutral B decays. The errors are statistical.

q^2 range (GeV^2)	$\Delta \mathcal{B}_\pi$ (10^{-4})	ϵ_π (%)	q^2 range (GeV^2)	$\Delta \mathcal{B}_\rho$ (10^{-4})	ϵ_ρ (%)
0–5	0.30 ± 0.05	2.1	0–10	0.73 ± 0.17	0.70
5–10	0.32 ± 0.05	2.9			
10–15	0.23 ± 0.05	3.8	10–15	0.82 ± 0.10	0.97
15–20	0.27 ± 0.05	3.5	15–25	0.59 ± 0.07	0.44
20–25	0.26 ± 0.03	3.3			
0–25	1.38 ± 0.10	3.1	0–25	2.14 ± 0.21	0.72

is a normalization factor, and α is a shape parameter. Since we cannot measure the normalization, only α is meaningful. Leaving both c_B and α free, we fit $\alpha = 0.61 \pm 0.09$, in agreement with LQCD results [5,6]. For decays to vector mesons, there are three form factors. The experimental uncertainties for $B \rightarrow \rho \ell \nu$ are still too large to measure these. Thus we have to rely on theoretical predictions.

Figure 3 compares the q^2 distributions for $B \rightarrow \pi \ell \nu$ and $B \rightarrow \rho \ell \nu$ with the various form-factor calculations, which we implement by reweighting simulated signal events [15]. We use χ^2 probabilities to quantify the agreement: for $B \rightarrow \pi \ell \nu$ we obtain good agreement with the BK fit to the data, $P(\chi^2) = 35\%$; and the predictions of LCSR1 [3], 38%; LQCD1 [5], 14%; and LQCD2 [6], 35%; but only marginal agreement with the prediction of ISGW II [8], $P(\chi^2) < 1\%$. For $B \rightarrow \rho \ell \nu$ all calculations [4,8] are compatible with the data within the large experimental uncertainties.

The systematic errors in the extraction of the branching fractions are listed in Table II. The contributions from each q^2 interval are conservatively treated as fully correlated and added linearly to obtain the uncertainty of the total branching fractions. Part of the q^2 variation of the stated errors may be due to statistical variations in simulated samples.

Uncertainties in the simulation of the reconstruction of charged particles and photons are evaluated by varying the reconstruction efficiencies and the photon-energy resolution and are added in quadrature. In addition, most K_L^0 escape detection. The impact of K_L^0 interactions in the calorimeter is estimated by varying in simulation their detection efficiency and energy deposition. To assess the uncertainty of the K^0 production rate, we vary the inclusive branching fractions of $D^+ \rightarrow \overline{K}^0 X$, $D^0 \rightarrow \overline{K}^0 X$, and $D_s^+ \rightarrow \overline{K}^0 X$ within their published errors [16]. All these constitute the total uncertainty of the neutrino reconstruction, which is dominant. For lepton identification we use relative un-
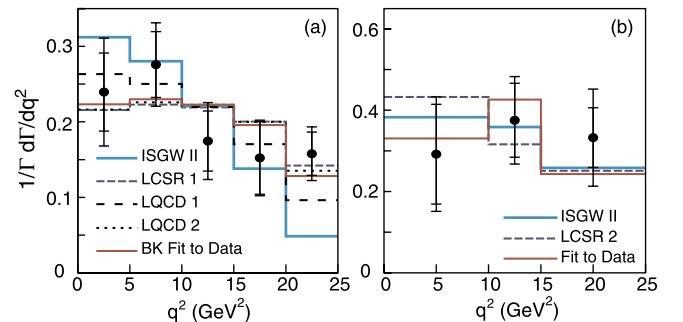

FIG. 3 (color online). Comparison of the differential decay rates as functions of q^2 for $B \rightarrow \pi \ell \nu$ (a) and $B \rightarrow \rho \ell \nu$ (b) with various form-factor predictions. The data are background subtracted and corrected for efficiency and radiative effects. The error bars are statistical (inner) and statistical plus systematic (outer).

TABLE II. Relative systematic uncertainties of the partial and total branching fractions $\mathcal{B}(B^0 \to \pi^- \ell^+ \nu)$ $(\Delta\mathcal{B}_\pi)$ and $\mathcal{B}(B^0 \to \rho^- \ell^+ \nu)$ $(\Delta\mathcal{B}_\rho)$ in the various q^2 bins. The total uncertainty in each column is the sum in quadrature of the listed contributions.

| q^2 range (GeV^2) | $\delta\Delta\mathcal{B}_\pi/\Delta\mathcal{B}_\pi$ (%) | | | | | | $\delta\Delta\mathcal{B}_\rho/\Delta\mathcal{B}_\rho$ (%) | | | |
	0–5	5–10	10–15	15–20	20–25	0–25	0–10	10–15	15–25	0–25
Track and photon reconstruction	7.4	5.7	9.2	3.5	8.7	6.8	16.7	10.8	15.9	14.2
K_L^0 Production and interactions	8.8	5.0	7.3	2.5	4.8	5.7	12.7	4.7	10.9	9.1
Lepton identification	2.3	2.3	2.3	2.3	2.3	2.3	2.3	2.3	2.3	2.3
$B \to X_c\ell\nu$ background	5.0	3.9	3.9	4.3	3.6	4.2	7.2	1.8	3.8	4.2
$B \to X_u\ell\nu$ background	0.5	1.5	0.6	2.2	5.7	2.1	10.9	9.1	19.2	12.5
Non-$B\overline{B}$ background	13.5	2.4	1.0	2.2	7.8	5.6	11.2	0.9	1.6	4.6
$N_{B\overline{B}}$	1.1	1.1	1.1	1.1	1.1	1.1	1.1	1.1	1.1	1.1
B lifetimes	1.1	1.4	0.2	0.5	2.1	1.1	0.7	0.6	0.9	0.7
f_{+-}/f_{00}	0.7	0.8	0.3	0.4	1.0	0.7	1.6	0.6	0.4	0.9
Isospin breaking	0.1	1.1	1.8	0.1	0.1	0.6	6.4	4.5	0.9	4.2
Radiative corrections	0.8	0.3	0.2	0.3	1.5	0.6	0.5	0.1	0.9	0.5
Total error	18.7	9.5	12.8	7.3	14.8	11.8	28.1	15.9	27.7	22.5

certainties of $\pm 2\%$ and $\pm 4\%$ for electrons and muons, respectively.

The uncertainty of the $B \to X_c\ell\nu$ background is evaluated by varying the $B \to D/D^*/D^{**}\ell\nu$ branching fractions [16] and the $B \to D^*\ell\nu$ form factors [17]. For the $B \to X_u\ell\nu$ background, we independently vary the branching fractions of $B^+ \to \omega\ell^+\nu$ and $B^+ \to \eta\ell^+\nu$ within their published errors [16,18]. We assume equal branching fractions for $\eta\ell\nu$ and $\eta'\ell\nu$ and use a relative uncertainty of 100% for the latter. We also vary the nonresonant contribution within the range allowed by the uncertainty of the total $B \to X_u\ell\nu$ branching fraction [19]. The impact of quark-hadron duality violation or weak annihilation effects have not been considered. We estimate the uncertainty of the small remaining non-$B\overline{B}$ background by comparing simulation with off-resonance data and extract a normalization error of $^{+70}_{-25}\%$ for electrons and $\pm 25\%$ for muons.

The overall uncertainty of the number of produced B mesons is 1.1%. We take into account the uncertainties of the ratio of B lifetimes, $\tau_{B^\pm}/\tau_{B^0} = 1.081 \pm 0.015$ [16], the charged-to-neutral B production ratio $f_{+-}/f_{00} = 1.044 \pm 0.050$ [16], and the potential effect of isospin breaking due to ρ^0–ω mixing [20]. We assign an uncertainty of 20% to the radiative corrections based on PHOTOS [21].

The impact of the uncertainties of the $B \to \pi\ell\nu$ form-factor shape on the measured branching fractions is negligible, whereas for the different $B \to \rho\ell\nu$ form-factor calculations we see variations of up to $\pm 6\%$ in $\mathcal{B}(B^0 \to \pi^- \ell^+ \nu)$ and $\pm 13\%$ in $\mathcal{B}(B^0 \to \rho^- \ell^+ \nu)$. We take the full spread between calculations as the uncertainty of the q^2 dependence of the form factors.

We extract $|V_{ub}|$ (see Table III) from the partial branching fractions $\Delta\mathcal{B}$ using the relation $|V_{ub}| = \sqrt{\Delta\mathcal{B}/(\tau_{B^0}\Delta\zeta)}$, where $\tau_{B^0} = (1.536 \pm 0.014)$ ps [16] is the B^0 lifetime and $\Delta\zeta$ denotes the predicted form-factor normalization in each q^2 interval. For $q^2 < 15$ GeV^2 we

derive $|V_{ub}|$ using LCSR calculations; for $q^2 > 15$ GeV^2 we use unquenched LQCD. To extract $|V_{ub}|$ from this measurement over the whole q^2 range, we extrapolate the LQCD results to low q^2 using the fits of the BK parametrization in Ref. [5,6] and the LCSR results to high q^2 using the parametrization given in Ref. [3]. We adopt the uncertainties of the form-factor normalization estimated in Refs. [3–6].

In conclusion, we have measured the exclusive branching fractions $\mathcal{B}(B^0 \to \pi^- \ell^+ \nu)$ and $\mathcal{B}(B^0 \to \rho^- \ell^+ \nu)$ as a function of q^2, and have extracted $|V_{ub}|$ using recent form-factor calculations. We measure the total branching fractions,

TABLE III. $|V_{ub}|$ derived for $B \to \pi\ell\nu$ and $B \to \rho\ell\nu$ signal for various q^2 regions and form-factor (FF) calculations: LCSR1 [3], LQCD1 [5], LQCD2 [6], LCSR2 [4], ISGW II [8]. For the cross feed from the other mode, we have used the BK fit to data for $\pi\ell\nu$ and LCSR2 for $\rho\ell\nu$. Quoted errors are statistical, experimental systematic, uncertainties of form-factor shape and form-factor normalization $\Delta\zeta$ (no form-factor normalization uncertainties are available for $\rho\ell\nu$).

	q^2 range (GeV^2)	$\Delta\zeta$ (ps^{-1})	$|V_{ub}|$ (10^{-3})
π FF			
LCSR1	0–15	5.1 ± 1.3	$3.27 \pm 0.16 \pm 0.19 \pm 0.10^{+0.53}_{-0.36}$
LQCD1	15–25	1.5 ± 0.4	$4.92 \pm 0.25 \pm 0.29 \pm 0.15^{+0.76}_{-0.52}$
LQCD2	15–25	2.0 ± 0.5	$4.16 \pm 0.22 \pm 0.24 \pm 0.12^{+0.72}_{-0.47}$
LCSR1	0–25	7.7 ± 2.3	$3.40 \pm 0.13 \pm 0.20 \pm 0.10^{+0.67}_{-0.42}$
LQCD1	0–25	5.7 ± 1.7	$4.00 \pm 0.14 \pm 0.23 \pm 0.12^{+0.78}_{-0.49}$
LQCD2	0–25	6.1 ± 2.1	$3.82 \pm 0.14 \pm 0.22 \pm 0.11^{+0.88}_{-0.52}$
ρ FF			
LCSR2	0–15	12.7	$2.82 \pm 0.18 \pm 0.30 \pm 0.18$
ISGW II	0–25	14.2	$2.91 \pm 0.12 \pm 0.33 \pm 0.19$
LCSR2	0–25	17.2	$2.85 \pm 0.14 \pm 0.32 \pm 0.19$

$$\mathcal{B}(B^0 \rightarrow \pi^- \ell^+ \nu) = (1.38 \pm 0.10 \pm 0.16 \pm 0.08) \times 10^{-4},$$

$$\mathcal{B}(B^0 \rightarrow \rho^- \ell^+ \nu) = (2.14 \pm 0.21 \pm 0.48 \pm 0.28) \times 10^{-4},$$

where the errors are statistical (data and simulation), experimental systematic, and uncertainties of the form-factor shapes. As a consistency check, we have also measured the branching fractions for the charged and neutral $\pi \ell \nu$ samples separately, $\mathcal{B}(B^0 \rightarrow \pi^- \ell^+ \nu) = (1.41 \pm 0.17 \pm 0.17 \pm 0.08) \times 10^{-4}$, $\mathcal{B}(B^+ \rightarrow \pi^0 \ell^+ \nu) = (0.70 \pm 0.10 \pm 0.08 \pm 0.04) \times 10^{-4}$. The ratio $\Gamma(B^0 \rightarrow \pi^- \ell^+ \nu)/\Gamma(B^+ \rightarrow \pi^0 \ell^+ \nu) = 2.21 \pm 0.41$ is consistent with the assumed isospin relation within the quoted statistical uncertainty.

For $B \rightarrow \pi \ell \nu$, the q^2 distribution agrees well with calculations based on LCSR [3] and unquenched LQCD [5,6], but the data disfavor ISGW II [8]. Instead of averaging results based on different calculations, we choose the measured form-factor shape and normalization of LQCD2 and quote

$$|V_{ub}| = (3.82 \pm 0.14 \pm 0.22 \pm 0.11^{+0.88}_{-0.52}) \times 10^{-3},$$

where the additional fourth error reflects the uncertainty of the form-factor normalization. The results are consistent with previous measurements [22,23], but have higher statistical accuracy, are less dependent on theoretical form-factor predictions, and benefit from recent advances in theoretical calculations [3–6].

[1] M. Kobayashi and T. Maskawa, Prog. Theor. Phys. **49**, 652 (1973).
[2] Charge-conjugate modes are included implicitly.
[3] P. Ball and R. Zwicky, Phys. Rev. D **71**, 014015 (2005).
[4] P. Ball and R. Zwicky, Phys. Rev. D **71**, 014029 (2005).
[5] J. Shigemitsu *et al.*, in *Proceedings of the 22nd International Symposium on Lattice Field Theory (Lattice 2004), Batavia, Illinois, 2004*, contributed paper, hep-lat/0408019.
[6] M. Okamoto *et al.*, Nucl. Phys. B Proc. Suppl. **140**, 461 (2005).
[7] B. Aubert *et al.* (*BABAR* Collaboration), Nucl. Instrum. Methods Phys. Res., Sect. A **479**, 1 (2002).
[8] D. Scora and N. Isgur, Phys. Rev. D **52**, 2783 (1995).
[9] F. De Fazio and M. Neubert, J. High Energy Phys. 06 (1999) 017.
[10] All variables denoted with a star (e.g. p^*) are given in the $\Upsilon(4S)$ rest frame; all others are given in the laboratory frame.
[11] These efficiencies and signal yields depend upon q^2-dependent form factors which, unless otherwise stated, are fit to the data for $B \rightarrow \pi \ell \nu$ and calculated using LCSR [4] for $B \rightarrow \rho \ell \nu$.
[12] R. J. Barlow and C. Beeston, Comput. Phys. Commun. **77**, 219 (1993).
[13] B. Aubert *et al.* (*BABAR* Collaboration), Phys. Rev. Lett. **93**, 011803 (2004).
[14] D. Becirevic and A. B. Kaidalov, Phys. Lett. B **478**, 417 (2000).
[15] D. Côté *et al.*, Eur. Phys. J. C **38**, 105 (2004).
[16] S. Eidelman *et al.* (Particle Data Group), Phys. Lett. B **592**, 1 (2004).
[17] B. Aubert *et al.* (*BABAR* Collaboration), in *Proceedings of the International Conference on High Energy Physics, Beijing, 2004*, contributed paper, hep-ex/0409047.
[18] C. Schwanda *et al.* (Belle Collaboration), Phys. Rev. Lett. **93**, 131803 (2004).
[19] B. Aubert *et al.* (*BABAR* Collaboration), Phys. Rev. Lett. **92**, 071802 (2004).
[20] J. L. Diaz-Cruz, G. Lopez Castro, and J. H. Munoz, Phys. Rev. D **54**, 2388 (1996); G. Lopez Castro, J. H. Munoz, and G. Toledo Sanchez, Phys. Rev. D **56**, 6025 (1997).
[21] E. Richter-Was *et al.*, Phys. Lett. B **303**, 163 (1993).
[22] S. B. Athar *et al.* (CLEO Collaboration), Phys. Rev. D **68**, 072003 (2003).
[23] B. Aubert *et al.* (*BABAR* Collaboration), Phys. Rev. Lett. **90**, 181801 (2003).